PAYLOAD POINTING AND ACTIVE VIBRATION ISOLATION USING HEXAPOD PLATFORMS

Hong-Jen Chen[*], Ronald M. Bishop, Jr.[†], and Brij N. Agrawal[‡]

This paper presents the recent implementation of pointing and vibration isolation techniques on hexapods at the Spacecraft Research and Design Center (SRDC) of Naval Postgraduate School (NPS). The center has two hexapod platforms: Ultra Quiet Platform (UQP) and Precision Pointing Hexapod (PPH). For vibration isolation, the Multiple Error Least Mean Square (LMS) Algorithm, the Clear Box Algorithm, and the Adaptive Disturbance Canceller have been implemented on either or both platforms and several enhancements have been made to various versions of the Clear Box Algorithm. All algorithms – including the Multiple Error LMS Algorithm, the Time Domain Clear Box Sin/Cosine Algorithm, the Time Domain Clear Box Adaptive Basis Algorithm, the Frequency Domain Clear Box Algorithm, and Adaptive Disturbance Canceller algorithm – achieved under various situations the performance as good as nearly two orders of magnitude on the reduction of narrowband vibrations. The theories of these vibration isolation algorithms and a simple yet effective compensator for the hexapod pointing are presented with experimental results. The advantages, the disadvantages, and the conditions under which each vibration isolation algorithm may be best applied were also given.

1. INTRODUCTION

Many future imaging spacecraft demand high pointing accuracy and low jitter requirement for the optical payload. It has become a more and more challenging problem on future space missions as the performance requirements of low vibration for the payloads keeps raising while the vibration sources on the spacecraft are increasing due to larger and larger flexible structures. Examples of such devices as the vibration sources include cryo-coolers, fluid pumps and other mechanical devices, in addition to reaction wheels and solar array drives. The need to develop improved techniques for vibration isolation has been recognized for more than a decade by several organizations such as NASA and USAF. These organizations initiated several research programs in this area to develop improved techniques and validate them by ground and in-orbit experiments.

While passive isolation presents a reliable, low cost solution that is effective for attenuating broadband high frequency vibrations, it is in general not suited for low frequency vibration isolation since the resulting mechanism is usually too soft to withstand the launch environment. Since a spacecraft has low frequency vibrations due to the excitation of flexible structures and the rotating devices, such as solar array drives, cryo-pumps, and reaction wheels, active techniques for low frequency vibration isolation is a desirable approach.

[*] Ph.D., US National Research Council Associate Fellow. Department of Aeronautics and Astronautics, Naval Postgraduate School, 699 Dyer Road, Room 137, Monterey, CA 93943-5106, hchen@nps.navy.mil
[†] Master Student, Naval Postgraduate School and Lieutenant Commander, United States Navy
[‡] Distinguished Professor and Director, Spacecraft Research and Design Center, Naval Postgraduate School, Monterey, CA, agrawal@nps.navy.mil

			Form Approved
Report Documentation Page			OMB No. 0704-0188

Public reporting burden for the collection of information is estimated to average 1 hour per response, including the time for reviewing instructions, searching existing data sources, gathering and maintaining the data needed, and completing and reviewing the collection of information. Send comments regarding this burden estimate or any other aspect of this collection of information, including suggestions for reducing this burden, to Washington Headquarters Services, Directorate for Information Operations and Reports, 1215 Jefferson Davis Highway, Suite 1204, Arlington VA 22202-4302. Respondents should be aware that notwithstanding any other provision of law, no person shall be subject to a penalty for failing to comply with a collection of information if it does not display a currently valid OMB control number.

1. REPORT DATE **APR 2003**	2. REPORT TYPE	3. DATES COVERED **00-00-2003 to 00-00-2003**

4. TITLE AND SUBTITLE **Payload Pointing and Active Vibration Isolation Using Hexapod Platforms**	5a. CONTRACT NUMBER
	5b. GRANT NUMBER
	5c. PROGRAM ELEMENT NUMBER
6. AUTHOR(S)	5d. PROJECT NUMBER
	5e. TASK NUMBER
	5f. WORK UNIT NUMBER
7. PERFORMING ORGANIZATION NAME(S) AND ADDRESS(ES) **Naval Postgraduate School,Department of Aeronautics and Astronautics,Monterey,CA,93943**	8. PERFORMING ORGANIZATION REPORT NUMBER
9. SPONSORING/MONITORING AGENCY NAME(S) AND ADDRESS(ES)	10. SPONSOR/MONITOR'S ACRONYM(S)
	11. SPONSOR/MONITOR'S REPORT NUMBER(S)

12. DISTRIBUTION/AVAILABILITY STATEMENT
Approved for public release; distribution unlimited

13. SUPPLEMENTARY NOTES

14. ABSTRACT

15. SUBJECT TERMS

16. SECURITY CLASSIFICATION OF:			17. LIMITATION OF ABSTRACT	18. NUMBER OF PAGES	19a. NAME OF RESPONSIBLE PERSON
a. REPORT **unclassified**	b. ABSTRACT **unclassified**	c. THIS PAGE **unclassified**	**Same as Report (SAR)**	**19**	

Standard Form 298 (Rev. 8-98)
Prescribed by ANSI Std Z39-18

Active vibration isolation allows significant performance enhancements over passive methods, but requires sensors, actuators, and processors, which must be reliable and efficient in mass and power consumption. However, with the development of smart sensors and actuators and the availability of powerful microprocessors, active vibration is becoming an attractive choice for vibration isolation. Active Control techniques for rejection of disturbances are numerous and include classical feedback, modern feedback, disturbance accommodating control, disturbance observers, repetitive control, adaptive control, adaptive inverse control, adaptive feed forward control, and neural networks [1]. In most cases, narrowband vibrations (periodic disturbances) are most effectively controlled through the use of feed forward techniques.

A widely used adaptive feed forward method for noise and vibration control is the Filtered-x LMS algorithm [2], or a Multi-Input Multi-Output (MIMO) implementation of it called the Multiple Error LMS algorithm [3]. A drawback of these methods is that they require a separately measured disturbance-correlated reference signal, which is adaptively filtered to form the control signal. LMS-derived methods also require prior knowledge of the system dynamics, which may vary with time. An algorithm named Adaptive Disturbance Canceller which is computationally efficient works similarly in suppressing static disturbance frequencies. This technique, however, possess the same disadvantage of needing a priori knowledge of the fixed frequencies. It also requires a disturbance measuring devices and an additional frequency identification algorithm if they vary during the entire process effectively, and therefore its computational advantage is partially or completely offset. A new technique that addresses these issues, is called the Clear Box Algorithm and approaches the control problem from a system identification perspective [4,5]. Using only knowledge of the actuator inputs and disturbance-corrupted sensor outputs, it allows the identification of both the system dynamics and the disturbance frequencies, and then uses the information to cancel the disturbance. Therefore this technique has the advantage that it does not need a disturbance-correlated signal.

At the Spacecraft Research and Design Center (SRDC) of Naval Postgraduate School, active vibration isolation by using smart struts is an active area of research. For the problems of precision payload pointing, tracking and vibration isolation, a hexapod platform with advanced active control is a promising device. Our center has two hexapod platforms: Ultra Quiet Platform (UQP) and Precision Positioning Hexapod (PPH). We first started the research on vibration isolation using UQP since this platform, having piezoelectric actuators, was designed explicit for such purpose only. The second platform at the center, PPH, is built with voice coil actuators and significantly larger actuation range; therefore it is equipped with the additional capability of payload pointing. Our research emphasis has since been placed more on the technology of pointing with simultaneous vibration isolation. This paper presents all our center's analytical and experimental efforts to meet requirement of fine pointing in the presence of vibration disturbance using hexapod platforms. Experimental results of pointing and vibration isolation are presented along with the assessment to the advantages, the disadvantages, and the conditions under which each vibration isolation algorithm can be best applied.

2. EXPERIMENTAL PLATFORMS

2.1 Ultra Quiet Platform (UQP)

The Ultra Quiet Platform as shown in Figure 1, is used for testing control algorithms for the vibration isolation of an imaging payload from spacecraft. It is configured similar to a "cubic" Stewart Platform where the struts are arranged as if they were on the edges of a cube, providing three orthogonal pairs of actuators.

In such arrangements, control in six degrees of freedom is possible using linear actuators and the coupling between actuators is minimized. The UQP is mounted on a spacecraft mockup, to which is mounted the disturbance source. The entire experiment sits on sixteen rubber feet attached to a 3800 lb RS4000 Optical Table (Newport Corporation) which uses four I-2000 Series Pneumatic Isolators (Newport Corporation) to
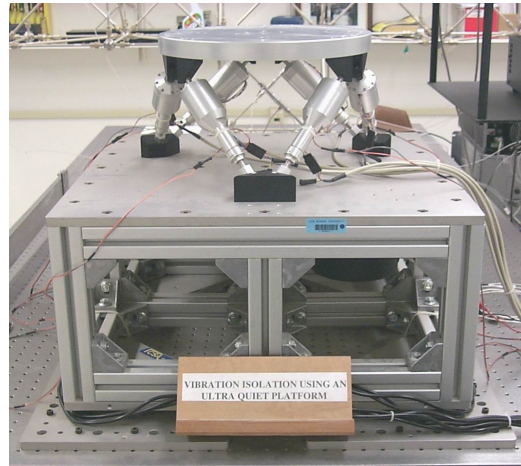
Figure 1 Ultra Quiet Platform (UQP) and Satellite Bus Mockup

help further isolate the experiment from floor vibration.

Each strut consists of a piezoceramic stack actuator (PZT) and a geophone sensor. The PZT converts control signal voltages to physical movement of the strut. The maximum displacement of the actuator is 50 μm, which is sufficient for vibration applications, but not for platform pointing or steering. The GS-11D Rotating Coil Geophone sensors (Geo Space) consists of wire coils supported by soft springs under the influence of a magnetic field, which provides a signal proportional to velocity. The source of disturbance for the disturbance rejection experiment, an AST-1B-4 Bass Shaker (Aura Systems) delivers peak force of 89 N whose resonance frequency is around 40 Hz.

2.2 Precision Pointing Hexapod (PPH)

This experimental platform is used for testing control algorithms for both vibration isolation of an imaging payload and fine steering. The Precision Pointing Hexapod, as shown in Figure 2, is based on an arrangement of six self-supporting electromagnetic voice coil actuators with in-line accelerometers that could enable control of higher vibration. Lower frequency steering and vibration isolation is provided by the use of laser/photo-diode based 2-axis position detecting system and eddy current position sensors. The system is capable of delivering significant range of motion in all 6 degrees of rigid body motion. It delivers over 5.7 mm of axial/position travel, 20 mm of lateral motion, 2.5 degree of tilt motion and 10 degree of twist.
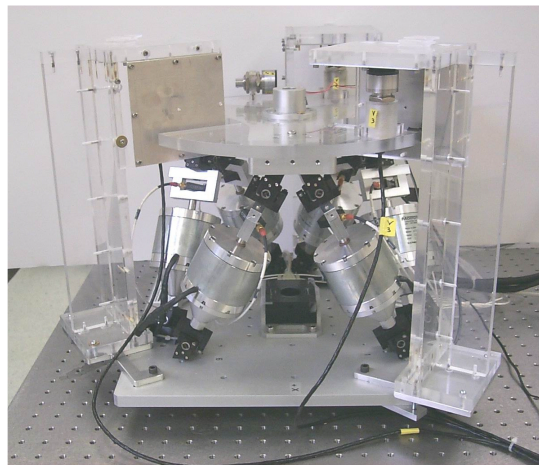

Figure 2 Precision Pointing Hexapod (PPH)

3. CONTROL ALGORITHMS

The current focus of the active vibration isolation for the spacecraft at the SRDC of NPS is the rejection of narrowband periodic disturbances. Adaptive feedforward algorithms, such as the widely used Multiple Error Least Mean Square Algorithm, the fairly recent Clear Box Algorithm, and the computationally efficient Adaptive Disturbance Canceller, can be used to cancel such disturbances more effectively than the traditional feedback control methods. These algorithms with some enhancement were implemented in full MIMO manner due to the nature of our experimental platforms. In this section the theories of these algorithms are outlined and the foundation of the two enhancement made to the Clear Box Algorithm are also laid out.

3.1 Multiple Error Least Mean Square (LMS) Algorithm

The Least Mean Square (LMS) algorithm uses an nth order digital FIR (Finite Impulse Response) filter to generate a feed forward control signal $y(k)$ and minimize the mean square error of, $\varepsilon(k)$, which represents the difference between $y(k)$ and the disturbance signal $d(k)$. The algorithm requires a "reference signal" $x(k)$ that is correlated with the disturbance signal $d(k)$ in order for the controller to perform well. The LMS algorithm acts to minimize $\varepsilon(k)$ by directing the filter coefficients towards the minimum point of a (quadratic) performance surface of $\varepsilon(k)$.

The block diagram of Multiple Error LMS algorithm is shown in Figure 3. We assume that there are M actuators and L sensors. There is a reference signal $x(k)$ which passes through a "primary plant" (P_1) before being sensed at the system output as $d(k)$. The disturbance at the lth sensor is represented by $d_l(k)$.
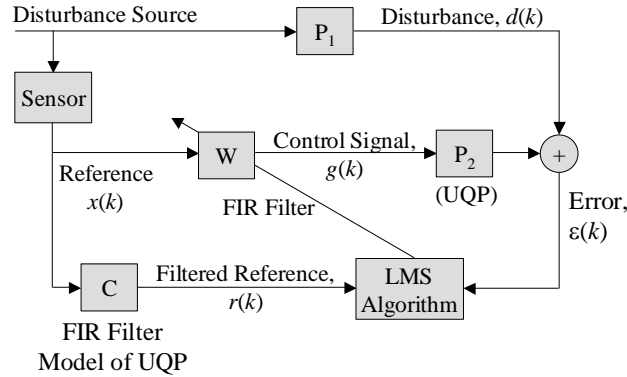

Figure 3 Multiple Error LMS Algorithm

The plant model used to filter the reference signal is a Jth order Finite Impulse Response (FIR) filter, C, whose coefficients c_{lmj} indicate the jth coefficient ($j=1, \ldots, J$) for the filter that models the dynamics between the mth actuator and the lth sensor. The resulting filtered signal, $r(k)$, includes $L \times M$ elements similarly indicated by $r_{lm}(k)$. The M control signals in $g(k)$ are generated by filtering the reference signal with an Ith order FIR filter W whose coefficients are w_{mi}. Finally, the error signal at each of the L sensors is indicated by $\varepsilon_l(k)$, an expression for which is

$$\varepsilon_l(k) = d_l(k) + \sum_{m=1}^{M} \sum_{j=0}^{J-1} c_{lmj} \sum_{i=0}^{I} w_{mi}(n-j)x(n-i-j) \tag{1}$$

As long as each $d_l(k)$ is partially correlated with $x(k)$ it is possible to reduce the error at each sensor through the proper choice of the coefficients w_{mi}. By defining the total error as

$$J = E\left\{\sum_{l=1}^{L}\varepsilon_l^2(k)\right\} \tag{2}$$

it is clear that J is a quadratic function of each of the coefficients w_{mi} w_{mi}, indicating that gradient descent methods allow convergence to the global minimum of J. The differentiation of J with respect to one coefficient is

$$\frac{\partial J}{\partial w_{mi}} = 2E\left\{\sum_{l=1}^{L}\varepsilon_l(k)\frac{\partial\varepsilon_l(k)}{\partial w_{mi}}\right\} \tag{3}$$

Differentiating Eq. (1) with respect to w_{mi} we obtain

$$\frac{\partial\varepsilon_l(k)}{\partial w_{mi}} = \sum_{j=0}^{J-1}c_{lmj}x(k-i-j) \tag{4}$$

The above signal is the same as that obtained by filtering the reference signal with the FIR filter, C, but delayed by i sample times. Denoting it (this filtered and delayed reference signal) by $r_{lm}(k-i)$, we have

$$\frac{\partial\varepsilon_l(k)}{\partial w_{mi}} = r_{lm}(k-i) \tag{5}$$

Adjusting each filter coefficient in w by the negative of the gradient expression in Eq. (3), and using the expression in Eq. (5), we obtain

$$w_{mi}(k+1) = w_{mi}(k) - 2\mu\sum_{l=1}^{L}\varepsilon_l(k)r_{lm}(k-i) \tag{6}$$

where μ is the adaptation rate.

Note that there is the assumption of time invariance in the w_{mi} filter coefficients and it is equivalent, in practice, to assuming that the filter coefficients change only slowly compared to the timescale of the response of the system to be controlled.

3.2 Time Domain Clear Box Algorithm

As mentioned earlier, two drawbacks of the Multiple Error LMS algorithm are the need of a disturbance correlated signal and the prior knowledge of the system to perform the disturbance rejection. The Clear Box Algorithm addresses both issues with the capability of complete identification of both the system and the unknown periodic disturbance, and then uses the obtained information to form the adaptive feedforward disturbance cancellation signal. For the development of the Clear Box Algorithm consider the following system

$$\begin{cases} x(k+1) = Ax(k) + Bu(k) + B_d d(k) \\ \quad y(k) = Cx(k) \end{cases} \tag{7}$$

where there are *m* inputs, *q* outputs, and *n* states. Thus $x(k)$ is an $n\times1$ state vector, $u(k)$ is an $m\times1$ input vector, and $y(k)$ is a $q\times1$ output vector. Similarly the system *A*, *B*, and *C* matrices have dimensions $n\times n$, $n\times m$, and $q\times n$, respectively. The system is represented in Figure 4. It is assumed that nothing is known except for the recorded system input $u(k)$, the disturbance-corrupted output data measurements $y(k)$, an upper bound on the true system order, *n*, and an upper bound on the number of frequencies, *f*, in the disturbance, $d(k)$.
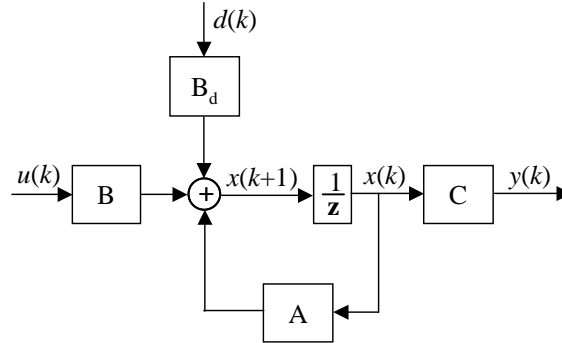

Figure 4 System Representation

By a process outlined in [1], the control (or excitation) input $u(k)$ and disturbance-corrupted output $y(k)$ satisfy a pth order input-output model,

$$
\begin{aligned}
y(k) &= \alpha_1 y(k-1) + \alpha_2 y(k-2) + ..\pm\alpha_p y(k-p) \\
&+ \beta_1 u(k-1) + \beta_2 u(k-2) + ..\pm\beta_p u(k-p)
\end{aligned}
\tag{8}
$$

as long as *p* is chosen to be sufficiently large such that

$$
p \geq \frac{n+2f+1}{q}
\tag{9}
$$

where the 1 accounts for a non-zero bias in the disturbance (if present). Notice that in this model the disturbance input $d(k)$ does not appear explicitly although it contributes to the data. Its information is completely absorbed in the coefficients α and β, which are referred to here as "disturbance-corrupted" coefficients.

Disturbance Identification through Modal Decomposition

To facilitate the removal of the disturbance modes it is convenient to convert the ARX (Auto-Regressive with eXogenous Input) model to an equivalent state space observable canonical form

$$
\begin{cases}
z(k+1) = A_p z(k) + B_p u(k) \\
\quad y(k) = C_p z(k)
\end{cases}
\tag{10}
$$

where

$$A_p = \begin{bmatrix} \alpha_1 & I & 0 & \cdots 0 \\ \alpha_2 & 0 & I & \ddots \vdots \\ \alpha_3 & 0 & 0 & \ddots 0 \\ \vdots & \vdots & \vdots & \ddots I \\ \alpha_p & 0 & 0 & \cdots 0 \end{bmatrix}, \qquad B_p = \begin{bmatrix} \beta_1 \\ \beta_2 \\ \beta_3 \\ \vdots \\ \beta_p \end{bmatrix},$$

$$C_p = \begin{bmatrix} I & 0 & 0 & \cdots 0 \end{bmatrix}$$

(11)

Conversion of this model to modal form yields the state space equations

$$\begin{cases} w(k+1) = \Lambda w(k) + \Gamma u(k) \\ \quad y(k) = \Omega w(k) \end{cases}$$

(12)

where Λ, Γ, and Ω are formed via similarity transformation;

$$\Lambda = T^{-1} A_p T, \qquad \Gamma = T^{-1} B_p, \qquad \Omega = C_p T$$

(13)

Typically, if p is chosen large enough, the damping ratios of the disturbance modes will be at least one or two orders of magnitude smaller than those of the noise modes or true system modes, and thus (the disturbance modes) can be easily identified. The frequencies are identified by monitoring the root of the polynomial and the accuracy of the identified frequency improves as p increases. Once the disturbance modes have been identified in the modal state space model, they can be selectively removed by eliminating the corresponding rows and columns from Λ, Γ, and Ω. The "disturbance-free" model is then converted to an equivalent ARX model with coefficients $\left[\bar{\alpha}_1, \bar{\alpha}_2, \ldots, \bar{\alpha}_p \right]$ and $\left[\bar{\beta}_1, \bar{\beta}_2, \ldots, \bar{\beta}_p \right]$. Thus the disturbance-corrupted output can be expressed as

$$\begin{aligned} y(k) &= \bar{\alpha}_1 y(k-1) + \bar{\alpha}_2 y(k-2) + ..\pm \bar{\alpha}_p y(k-p) \\ &+ \bar{\beta}_1 u(k-1) + \bar{\beta}_2 u(k-2) + ..\pm \bar{\beta}_p u(k-p) + \eta(k) \end{aligned}$$

(14)

where the right-hand side of Eq. (14) is driven by disturbance corrupted outputs. The disturbance effect, $\eta(k)$, can be calculated in real time by re-arranging Eq. (14) as

$$\begin{aligned} \eta(k) &= y(k) - \bar{\alpha}_1 y(k-1) - \bar{\alpha}_2 y(k-2) - ..\mp.\bar{\alpha}_p y(k-p) \\ &- \bar{\beta}_1 u(k-1) - \bar{\beta}_2 u(k-2) - ..\mp.\bar{\beta}_p u(k-p) \end{aligned}$$

(15)

At this point the disturbance-free system model and the disturbance effect are known and from Eq. (15), (setting all output $y(k)$ to zero,) the feedforward control $u_f(k)$, that cancels steady-state disturbances satisfies

$$\bar{\beta}_1 u_f(k-1) + \bar{\beta}_2 u_f(k-2) + ..\pm \bar{\beta}_p u_f(k-p) = -\eta(k)$$

(16)

Sine/Cosine Method

The Clear Box Algorithm takes advantage of the knowledge that the control signal, $u_f(k)$, needs to be made up of periodic components in order to cancel periodic disturbances. The first option for generating such a $u_f(k)$, as employed in [4], is to use a sine/cosine pair for each disturbance frequency. For L identified disturbances, the assumed form of the control signal

$$u_f(k) = \sum_{i=1}^{L} \left[a_i \cos(\omega_i k \Delta t) + b_i \sin(\omega_i k \Delta t) \right] \qquad (17)$$

is substituted into Eq. (16) and the resulting set of equations (linear in the coefficients a_i and b_i) is solved in real time using Recursive Least Squares (RLS), and employing a "forgetting factor" λ_f to weight recent data more heavily. The control signal in Eq. (17) is thus a combination of sine and cosine functions, whose L frequencies are estimated using methods outlined in the previous section.

Adaptive Basis Method

An alternative [6,7] to using the sine and cosine functions as the bases for synthesizing the disturbance rejection signal, $u_f(k)$, for the Clear Box Algorithm, is to use the N-sample shifted versions of the disturbance effect signal, $\eta(k)$..

For this "Adaptive Basis Method", the control signal is formed from $\eta(k)$ as follows

$$u_f(k) = \psi_1 \eta(k - \Delta_1) + \psi_2 \eta(k - \Delta_2) + .\pm \psi_N \eta(k - \Delta_N) \qquad (18)$$

where $N \geq 2f + 1$. The Δ_i values ($i = 1, ... N$) are the number of samples that the disturbance effect would shifted to generate each of the N basis functions that are linearly combined to form the control signal. Each Δ_i value is pre-selected by the operator, and the guidelines below should be followed.

$$\begin{aligned}
\Delta_i &\geq 1 & \forall\, i \\
\Delta_i &\neq \Delta_j & \forall\, i, j \\
\left| \Delta_i - \Delta_j \right| &\neq \left| \Delta_j - \Delta_k \right| & \forall\, i, j, k
\end{aligned} \qquad (19)$$

The first guideline prevents any problems with causality by using the disturbance effect that is delayed by at least one time sample. The second ensures that two functions do not have the same time shift (such a pair would be identical functions). The third introduces a random characteristic to the time shifting, and prevents linear dependence of the basis functions for any given disturbance frequency. The control coefficients in Eq.(18), ψ_i, where $i = 1, ... N$, are recursively estimated in the same manner as with the Sine/Cosine Method.

There are two basic advantages associated with the adaptive basis approach. First, it eliminates the need to estimate the disturbance frequencies. Second, since the disturbance effect signal $\eta(k)$ is calculated in real time, it contains the exact frequency content of the actual disturbances. Any change in the disturbance frequencies immediately appear in the disturbance effect signal, making the adaptive basis approach capable of handling time-varying disturbance frequencies.

3.3 Frequency Domain Clear Box Algorithm

The Frequency Domain Clear Box Algorithm [8] parallels the development of its time domain counterpart. It is the analog with two enhancements. First, a Phase Cancellation Repetitive Control Algorithm [9] is added to the process of generating feedforward cancellation signal. Zero tracking error, i.e. output error suppressed down to practically the background noise level, is produced through the integration action along repetitions. Second, when the situation of limited control authority is encountered, the yes-or-no decision algorithm on deciding which disturbance frequencies to control is replaced by a quadratic programming algorithm, which allows partial control of certain disturbance frequencies. Therefore actuator saturation is

avoided and the overall performance is improved. Computational efficiency is ensured by the application of FFT for this algorithm, but there are added difficulties in dealing with the noisy data, the leakage effect, and the synchronization issue of online system identification in the presence of periodic disturbances. The following two sections summarize the theoretical background of the enhancements that were made.

Phase Cancellation Repetitive Control

Consider the input-output relationship for the following general time invariant MIMO system:

$$\begin{cases} x(k+1) = Ax(k) + Bu(k) + w(k) \\ \quad y(k) = Cx(k) \end{cases} \tag{20}$$

where x is the state vector, u u is the batch mode repetitive control input vector adding to feedback control command to correct for repeating errors, y is the output vector, and w w includes repetitive disturbances as well as the initial command to the feedback controller, which are both of the same period, p. The system is assumed asymptotically stable and all eigenvalues of A A are less than one.

Take z-transform of Eqs. (20) and after combining terms, we obtain

$$Y(z) = G_c(z)U(z) + R_w(z) \tag{21}$$

where

$$G_c(z) = C(zI - A)^{-1}B$$
$$R_w(z) = C(zI - A)^{-1}W(z) \tag{22}$$

with I being the identity matrix with matching dimensions and $U(z)$ and $W(z)$ being the z-transforms of $u(k)$ and $w(k)$, respectively.
The z-transform version of the repetitive control law is

$$U_j(z) = U_{j-1}(z) + L(z)E_{j-1}(z) \tag{23}$$

where

$$E_{j-1}(z) = Y_d(z) - Y_{j-1}(z) \tag{24}$$

with j representing the repetition number (repetition 0 referring to the initial repetition with no modification to the feedback command), and $L(z)$ and $Y_d(z)$ representing the z-transforms of the time-domain learning coefficients and the desired output, respectively.

Applying Eqs. (21) and (23), after manipulations, one obtains

$$Y_j(z) = [I - L(z)G_c(z)]Y_{j-1}(z) + L(z)G_c(z)Y_d(z) \tag{25}$$

and

$$E_j(z) = [I - L(z)G_c(z)]E_{j-1}(z) \tag{26}$$

which relate the output and error profiles from one repetition to the next. Using recursive substitution in Eqs. (25) and (26) gives

$$Y_j(z) = [I - L(z)G_c(z)]^j Y_0(z) + \{I - [I - L(z)G_c(z)]^j\}Y_d(z) \tag{27}$$

and

$$E_j(z) = [I - L(z)G_c(z)]^j E_0(z) \tag{28}$$

where the subscript 0 indicates initial trail repetition.

It is then recognized that the condition needed for convergence to zero error is

$$|\lambda_i| < 1, \quad i = 1, 2, \dots, q \tag{29}$$

where λ_i's are the eigenvalues of $I - L(z)G_c(z)$ and q is the number of outputs. Considering steady-state frequency response, setting $z = e^{j\omega T}$ where T is the sample time, the learning therefore produces monotonic decay of every steady-state discrete frequency components of the error. For the case of SISO system, Eq. (29) reduces to

$$\left|1 - L(e^{j\omega T})G_c(e^{j\omega T}))\right| < 1, \quad i = 1, 2, \dots, q \tag{30}$$

This is a sufficient condition for convergence, and also a condition for good transients during the repetitive control process, producing monotonic convergence in steady-state response. Thus it is a performance condition that requires the Nyquist plot of $L(e^{j\omega T})G_c(e^{j\omega T})$ to be within a unit circle centered on the real axis at unit positive distance.

The phase cancellation repetitive control law, for the case of SISO system, is given as

$$L(e^{j\omega_k T}) = \begin{cases} -G_c(e^{j\omega_k T}), if \left|G_c(e^{j\omega_k T})\right| \leq 1 \\[2ex] -\dfrac{G_c(e^{j\omega_k T})}{\left|G_c(e^{j\omega_k T})\right|}, if \left|G_c(e^{j\omega_k T})\right| > 1 \end{cases} \tag{31}$$

where $\omega_k = \dfrac{2\pi k}{NT}$, $k = 0, 1, \dots, N-1$ and $G(e^{i\omega_k T})$ is the frequency response of the system at the N discrete frequencies ω_k's.

This repetitive control law actually puts all points on the Nyquist plot of $L(e^{j\omega T})G_c(e^{j\omega T})$ on the real axis between the origin and $+1$. Therefore it satisfies the unit circle performance condition (30) for all N discrete frequencies at ω_k's.

For a MIMO system with square and diagonalizable system frequency response function at every frequency, the learning gain matrix is

$$L(e^{j\omega_k T}) = V^{-1}(e^{j\omega_k T})\Lambda_L(e^{j\omega_k T})V(e^{j\omega_k T}) \tag{32}$$

where V and Λ_ϕ are the eigenvector and the eigenvalue matrices of the transfer matrix $G_c(e^{j\omega T})$, and the eigenvalues of the matrix Λ_L are

$$\lambda_i(e^{j\omega_k T}) = \begin{cases} -\lambda_i[G_c(e^{j\omega_k T})], if \left|\lambda_i[G_c(e^{j\omega_k T})]\right| \leq 1 \\[2ex] -\dfrac{\lambda_i[G_c(e^{j\omega_k T})]}{\left|\lambda_i[G_c(e^{j\omega_k T})]\right|}, if \left|\lambda_i[G_c(e^{j\omega_k T})]\right| > 1 \end{cases} \tag{33}$$

where $\omega_k = \dfrac{2\pi k}{NT}$, $k=0,1,\ldots,N-1$ and $i=0,1,\ldots,q$, and $G_c(e^{j\omega T})$ and $\lambda_i[G_c(e^{j\omega_k T})]$ are the frequency response of the system and its eigenvalues at all N discrete frequencies at ω_k's.

Intelligent Error Cancellation by Quadratic Programming

In Time Domain Clear Box Algorithms, the control computation gives full information as to how much control effort is required to cancel each frequency component of the error, but only yes or no decisions were made when full cancellation requires use of control actions that exceed the actuator limits. The application of quadratic programming to the worst case scenario of multiple disturbance frequencies allows partial cancellation that prevents actuator saturation and produces overall improvement on the tracking accuracy.

Consider a six-input, six-output system subject to the disturbance of five frequencies with limited control authority u_{max} for each input actuator. Let d_{ij} represent the amplitude of the disturbance frequency i on output j. and c_{ij} be the amplitude of the input signal needed to cancel d_{ij}. The maximum possible amplitude of the disturbance on output j is the sum of d_{ij} over i. It occurs when all five frequency components are at their peak values at the same time.

Also define
$\underline{d}_i$ and $\underline{c}_i$ as column vectors of d_{ij} and c_{ij},
α_i as the fraction of input ($0 \le \alpha_i \le 1$) to cancel the disturbance frequency i for all outputs,
β_i as compliment of α_i so that $0 \le \beta_i = 1 - \alpha_i \le 1$,
C, D, and $\underline{\beta}$ as column matrices of c_i, d_i, and β_i,
$\underline{1}_5$ and $\underline{1}_6$ as 5- and 6-dimensional column vectors with all entries equal to one,
$\underline{0}_6$ as 6-dimensional column vectors with all entries equal to zero,
and
u_{max} as the same saturation limit for all actuators.

Then the maximum disturbances vector is

$$\underline{d} = \underline{d}_1 + \underline{d}_2 + \underline{d}_3 + \underline{d}_4 + \underline{d}_5 \tag{34}$$

The maximum magnitude for each input is

$$\begin{aligned} \underline{c} &= \alpha_1 \underline{c}_1 + \alpha_2 \underline{c}_2 + \alpha_3 \underline{c}_3 + \alpha_4 \underline{c}_4 + \alpha_5 \underline{c}_5 \\ &= C(\underline{1}_5 - \underline{\beta}) \\ &\le u_{max} \underline{1}_6 \end{aligned} \tag{35}$$

and the maximum remaining disturbance after this fractional cancellation is

$$\underline{d} = \beta_1 \underline{d}_1 + \beta_2 \underline{d}_2 + \beta_3 \underline{d}_3 + \beta_4 \underline{d}_4 + \beta_5 \underline{d}_5 = D\underline{\beta} . \tag{36}$$

To optimize the amount of each mode to cancel, quadratic programming is used to minimize the objective function

$$J = \underline{d}^T \underline{d} = \underline{\beta}^T D^T D \underline{\beta} \tag{37}$$

with component-by-component inequality constraints

$$\underline{0}_6 \le \beta_i \le \underline{1}_6, \quad \forall i, \tag{38}$$

and

$$-C\underline{\beta} \le u_{max}\underline{1}_6 - C\underline{1}_5, \tag{39}$$

3.4 Adaptive Disturbance Canceller

The Adaptive Disturbance Canceller (ADC) implemented for the Precision Pointing Hexapod at NPS follows the same approach proposed in 1998 by Bertran and Mortoro [12]. This approach states that assuming the plant is linear and stable and has no zeros at the frequencies of interest, it is possible to generate an arbitrary sinusoidal at the output of the system to cancel any sinusoidal disturbance. Figure 5 is a block diagram illustrating this control approach.
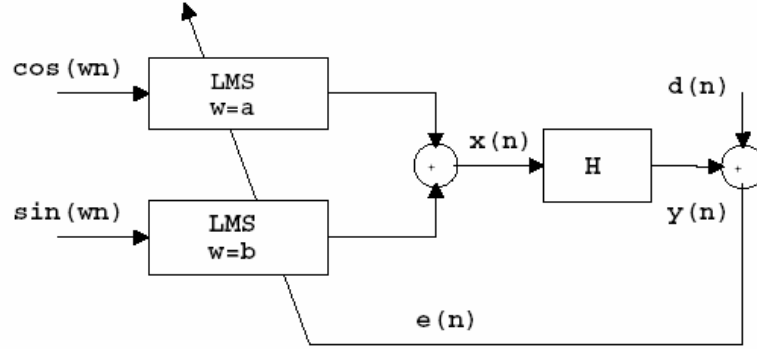
Figure 5 Adaptive Disturbance Canceller

Assuming the plant H is linear, for any sinusoidal signal $d[n]$ with frequency ω_c it is possible to find a sinusoidal input $x[n]$ such that $y[n] = -d_n$ (if $\mathcal{H}(e^{j\omega_c}) \ne 0$). This input can be written as:

$$x[n] = X\cos(\omega_c n + \beta_x) \tag{40}$$

There exist several algorithms for finding the optimal value of $x[n]$ to minimize the error, $e[n] = y[n] + d[n]$, assuming $y[n]$ is linear. Using this assumption, (40) can be changed to the equivalent form:

$$x[n] = a\cos(\omega_c n) + b\sin(\omega_c n) \tag{41}$$

Assuming that $\mathcal{H}(e^{j\omega_c}) = \alpha e^{j\beta}$, with α as the magnitude and β the phase, the steady-state output $y[n]$ can then be expressed as:

$$y[n] = a\alpha\cos(\omega_c n + \beta) + b\alpha\sin(\omega_c n + \beta) \tag{42}$$

Using this form the output $y[n]$ is linear in the parameters a and b, which can be found by an adaptive algorithm. The update equations given by Bertran and Montoro for these parameters are

$$a[n+1] = a[n] + \mu e[n]\cos(\omega_c n)$$
$$b[n+1] = b[n] + \mu e[n]\sin(\omega_c n) \tag{43}$$

where μ is a learning factor to be determined.

3.5 PID Hexapod Pointing Compensator

Our first pointing controller implemented PPH is a PID controller, whose performance will be taken as the baseline for comparison to those of more advance pointing controller in the future. As will be presented in the next result section, such simple compensator can produce sufficiently good performance, which is made possible by a Jocobian matrix that interprets commanded position and orientation of the hexapods to necessary strut/actuator displacements to accomplish the task. By the use of carefully constructed Jacobian matrix, the hexapod strut motions are well decoupled, and therefore can be controlled well by simple linear controllers. The Jacobian matrix implemented follows that was developed by Tsai [14]. It is a small motion approximation, which we applied to tasks around the hexapod's nominal neutral position such as tracking small straight line through origin or small circular motion about origin.

4. EXPERIMENTAL RESULTS

4.1 Vibration Isolation Test Results on the Ultra Quiet Platform

Three time-domain controllers, Multiple Error LMS Method, Clear Box Sine/Cosine Method, and Clear Box Adaptive Basis Method were tested for the vibration isolation of a disturbance frequency at 120 Hz on UQP. The experiments demonstrate [6,7] that all three controllers work effectively reducing the sensor output to the level of the background noise.

Next, the three controllers were tested for a single time-varying disturbance frequency with the profile shown in Figure 6.
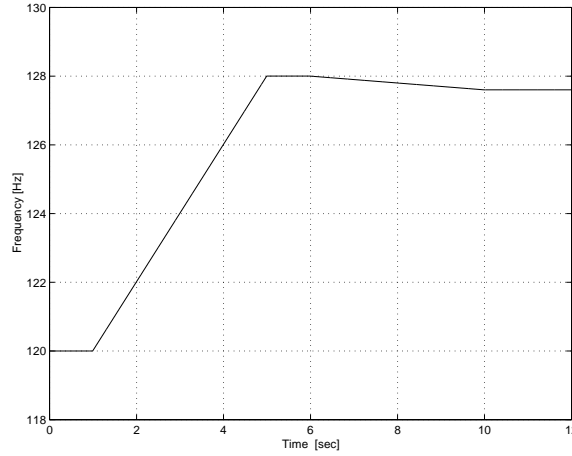

Figure 6 Frequency Variation Profile, Single Disturbance

With a good source of well-correlated disturbance signal $x(k)$, the Multiple Error LMS algorithm performs quite well over the course of the frequency variation profile as shown in Figure7.
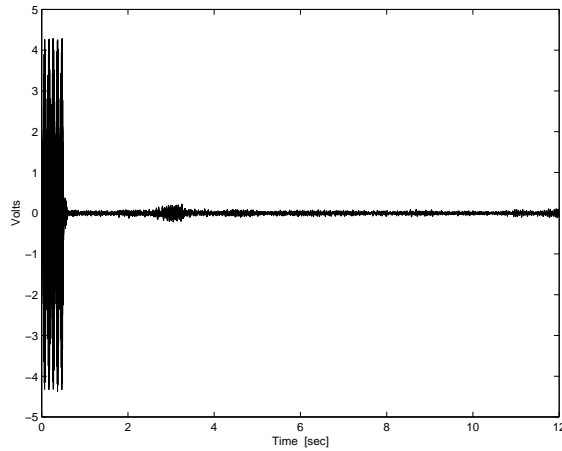
Figure 7 Uncontrolled response and Multiple Error LMS Method Response, One Varying Frequency

The performance of Clear Box/Sine Cosine Method is shown in Figure 8. This method had significant degradation in performance during rapid ramp-up in frequency since the frequency estimates (when updated through batch processing once per second) quickly become inaccurate.
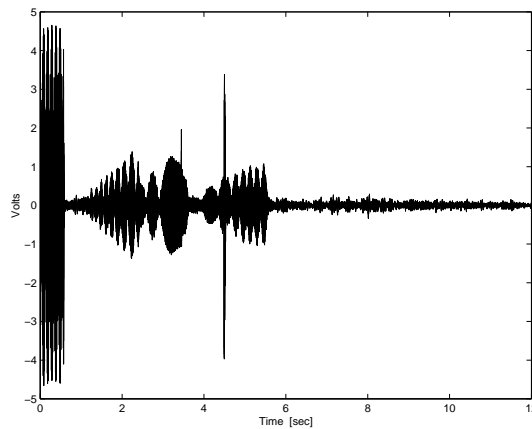

Figure 8 Uncontrolled response and Clear Box Sine/Cosine Method response, One Varying Frequency

The performance of Clear Box/Adaptive Method is shown in Figure 9. This method is able to maintain good performance, reducing the sensor output to the background noise level. Therefore, this method is effective even if the frequency of the disturbance is varying.
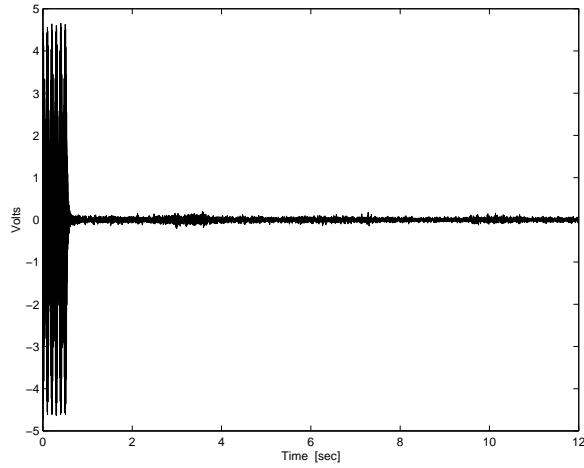
Figure 9 Uncontrolled response and Clear Box Adaptive Basis Method response, One Varying Frequency

Similar test cases were also run for the Frequency Domain Clear Box Algorithm implemented in batch mode. Comparable good final level was achieved for the case of time-invariant, single or multiple disturbance frequencies. The algorithm is less computational intensive than its time domain counterparts. It cancels, as shown in Figure 10, just as well a disturbance with 5 frequency components, which is already beyond the computational capacity of the control hardware for the Time-Domain Clear Box Method. But as the case of Time-Domain Clear Box/ Sine Cosine Method, it was unable to adaptive quickly to variable frequency profile since it was batch-implemented.
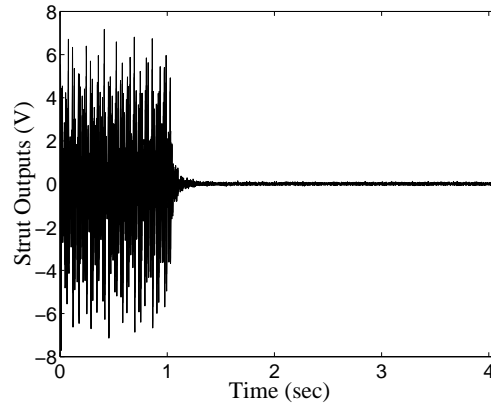

Figure 10 Uncontrolled response and MIMO controlled response of 5 disturbance frequencies (repetition 10)

4.2 Vibration Isolation Test Results on the Precision Pointing Hexapod

Figure 11 shows the vibration isolation test results when the Adaptive Disturbance Canceller is applied on the Precision Pointing Hexapod to suppress a disturbance with constant fundamental frequency at 50 Hz.

Due to the nonlinearity in the system, such as stick friction and ball joint clearance[1], three additional cancellers with individual adaptation process to those of the first three harmonics (100, 150, and 200 Hz) were also implemented. All four disturbance frequencies were practically suppressed to the ambient noise level. The adaptive disturbance cancellers are applied to each of the six struts of the hexapod in an identically, i.e. decentralized, manner.
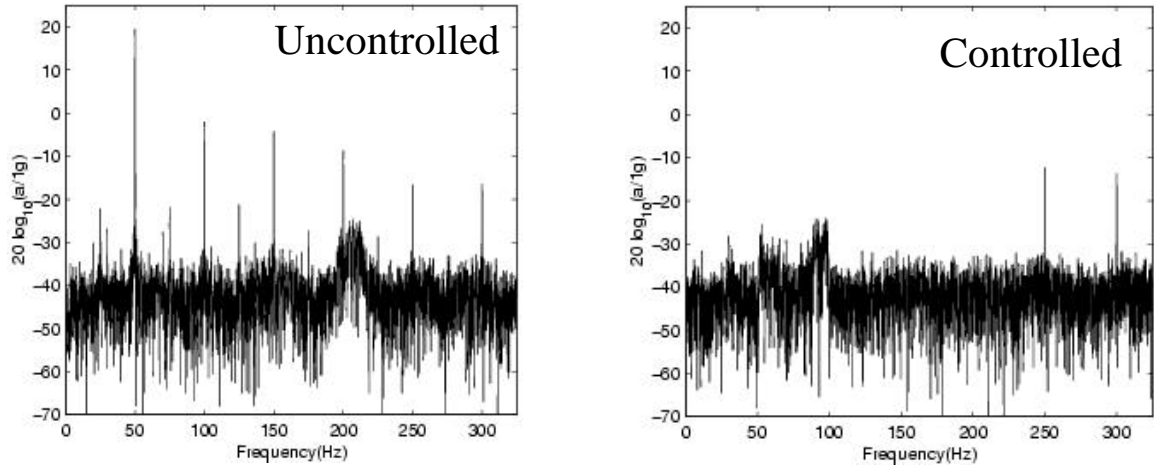

Figure 13 Uncontrolled response and Adaptive Disturbance Canceller response, One Static Fundamental Frequency at 50 Hz

4.3 Pointing Test Results on the Precision Pointing Hexapod

The hexapod tracking performance of rotating about either x or y axis, i.e. straight line tracking along y or x axis, is illustrated in Figure 12. The gains of the PID controller used are $K_p=2$, $K_i=6$, and $K_d=0.17$. The tracking errors were less than ±0.05 degree for rotations about either axis up to 1 degree, which was an order of magnitude improvement over the open loop case.
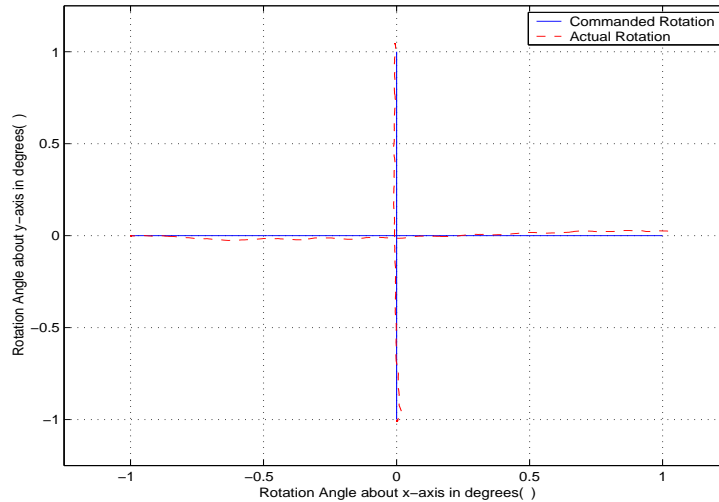

Figure 12 Tracking Errors Corresponding to Two Orthogonal Straight Line Trajectories (Rotations about x and y axes)

---

[1] Later on this problem was essentially eliminated by replacing ball joints with flexure joints, which is what is used for the pointing tests.

The performance of the hexapod tracking circles with different sizes (from 0.1 degree to 1 degree) and at different speed (from 0.1 Hz to 2 Hz) are also tested. Results in Figures 13 and 14 show that the circular tracking performance is indeed dependent on the sizes of the circle and the speed of tracking them. In general, the larger the circle or the faster the speed, the larger the error. However, when the tracking speed is quite slow, e.g. at 0.1 Hz, the performance seems to be much less sensitive to the size of the circle.
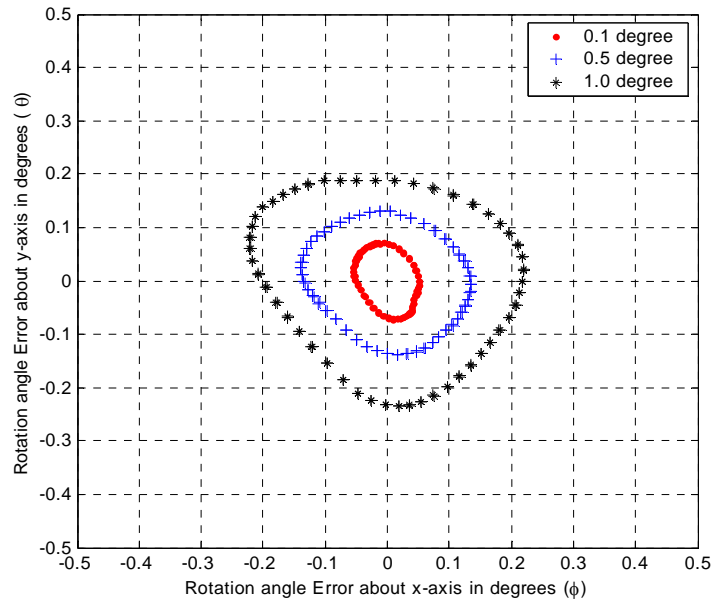

Figure 13 Tracking Errors Corresponding to 2.0 Hz Circular Trajectories for Various Radii
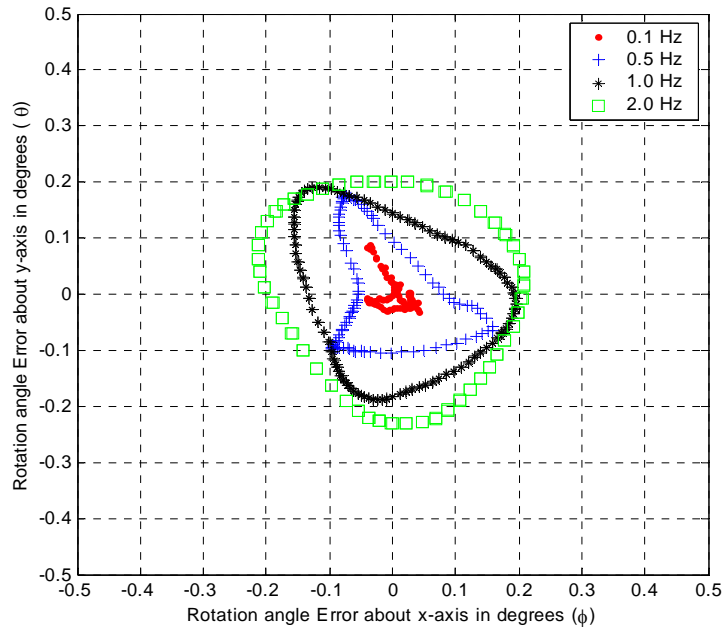

Figure 14 Tracking Errors Corresponding to Clockwise, 1.0° Radius, Circular Trajectories for Various Tracking Speeds

5. CONCLUSIONS

Based on the experimental results of vibration isolation on our two hexapod platforms UQP and PPH, we made the following conclusions. The drawbacks of the Multiple Error LMS Algorithm are that the tuning of the adaptation rate is necessary to achieve optimal convergence, and that it requires one or more disturbance correlated signals to perform the disturbance cancellation well. When the disturbance-correlated signals are available, it is the preferred control algorithm due to its better computational efficiency. The performance from the Clear Box method, implemented in either Time-Domain or Frequency Domain, meets or exceeds that of Multiple Error LMS Algorithm without requiring a measured disturbance-correlated signal. When there are no disturbance-correlated signals available, as is the case with majority of the systems, the Clear Box method is the method of choice since it is capable of doing on-line disturbance and system identification. The Time Domain Clear Box Sine/Cosine Method is preferred when the disturbance frequencies are time-independent or just varying slowly, but for rapidly varying disturbance frequencies, the Adaptive Basis version should be used as it provides better performance. Both of the time domain Clear Box versions have, however, the drawback of requiring significantly higher processing speed.

Base on the experimental results on pointing and vibration isolation on PPH, PID controller with a well constructed decoupling matrix provides adequate performance for pointing. A computation efficient Adaptive Disturbance Cancellation algorithm was tested and proved as effective as the vibration isolation algorithms mentioned above in suppressing constant disturbance frequencies. This technique, however, possess the same disadvantage of needing a priori knowledge of the fixed frequencies.

6. ACKNOWLEDGMENTS

7. REFERENCES

1. Goodzeit, N.E., *System and Disturbance Identification for Adaptive Disturbance-Rejection Control*, Ph.D. Dissertation #3019T, pp. 5-16, Department of Mechanical and Aerospace Engineering, Princeton University, Princeton, NJ, June 1998.

2. Elliott, S.J., Stothers, I.M., and Nelson, P.A., "A Multiple Error LMS Algorithm and Its Application to the Active Control of Sound and Vibration," IEEE Transactions on Acoustics, Speech, and Signal Processing Vol. ASSP-35, No. 10, pp. 1423-1434, October 1987.

3. Widrow, B. and Stearns, S.D., Adaptive Signal Processing, pp. 288-294, Prentice-Hall, Englewood Cliffs, New Jersey, 1985.

4. Goodzeit, N.E., and Phan, M.Q., "Exact System Identification in the Presence of Completely Unknown Periodic Disturbances," Department of Mechanical and Aerospace Engineering Technical Report No. 2096, Princeton University, January 1997, Princeton, NJ. Also, Journal of Guidance, Control, and Dynamics, Vol. 23, No.2, pp. 251-259, Mar/Apr 2000.

5. Goodzeit, N.E., and Phan, M.Q., "A Clear-Box Adaptive System for Flexible Spacecraft Identification and Disturbance Rejection," Journal of Vibration and Control, Vol. 6, No. 5; pp. 757-780, July 2000.

6. S.G. Edwards, B.N. Agrawal, M.Q. Phan, and R.W. Longman, "Disturbance Identification and Rejection Experiments on an Ultra Quiet Platform," Advances in the Astronautical Sciences, Vol. 103, 2000.

7. S. G. Edwards, Active *Narrowband Disturbance Rejection on an Ultra Quiet Platform*, Ph.D. Dissertation, Department of Aeronautic and Astronautic Engineering, Naval Postgraduate School, Monterey, CA, September 1999.

8. H.-J. Chen, R.W. Longman, B.N. Agrawal, and M.P. Phan,"FFT-Based Clear-Box Disturbance Rejection on an Untra Quiet Platform," Proceedings of the 10th AAS/AIAA Space Flight Mechanics Meeting, Clearwater, Florida, January 2000, Advance in the Astranautical Sciences, to appear

9. H. Elci, R.W. Longman, M.Q. Phan, J.-N. Juang, and R. Ugoletti, "Automated Learning Control Through Model Updating For Precision Motion Control," Adaptive Structures and Composite Materials: Analysis and Applications, AD-Vol. 45/MD-Vol. 54, ASME, Nov. 1994, pp. 299-314.

10. H.-J. Chen; B. N. Agrawal, R. W. Longman, M. Q. Phan, S. G. Edwards, "Rejection of Multiple Periodic Disturbances Using MELMS with Disturbance Identification," Advances in the Astronautical Sciences, v 108 I, 2001, Proceedings of the AAS/AIAA Space Flight Mechanics Meeting, Feb 11-15 2001, Santa Barbara, CA, p 587-606

11. H.-J. Chen, *Multiple Periodic Disturbance Rejection Techniques for Vibration Isolation*, Ph.D. Dissertation, Department of Mechanical Engineering, Columbia University, New York, NY, June 2001.

12. E. Bertran and G. Montoro, "Adaptive Suppression of Narrow-Band Vibrations, " in 5th International Workshop on Advanced Motion Control, pp. 288-292, June-July 1998.

13. C. G. Taranti, R. Cristi, and B. N. Agrawal, "An Efficient Algorithm for Vibration Suppression to Meet Pointing Requirements of Optical Payloads," AIAA Guidance, Navigation, and Control Conference & Exhibit, 6 - 9 Aug 2001, Montreal, Quebec, Canada

14. Ronald M. Bishop, Jr., *Development of Precision Pointing Controllers with and without Vibration Suppression for the NPS Precision Pointing Hexapod*, Master & Engineer's Thesis, Department of Aeronautic and Astronautic Engineering, Naval Postgraduate School, Monterey, CA, December 2002.

15. Lung-Wen Tsai, "Robot Analysis," John Wiley & Sons, Inc, 1999.